AFRL-RX-WP-JA-2015-0078

SEPARATING TEST ARTIFACTS FROM MATERIAL BEHAVIOR IN THE OXIDATION STUDIES OF HfB_2-SiC AT 2000°C AND ABOVE (POSTPRINT)

Michael K. Cinibulk
AFRL/RXCC

Carmen M. Carney and Triplicane A. Parthasarathy
UES, Inc.

FEBRUARY 2012
Interim Report

AIR FORCE RESEARCH LABORATORY
MATERIALS AND MANUFACTURING DIRECTORATE
WRIGHT-PATTERSON AIR FORCE BASE OH 45433-7750
AIR FORCE MATERIEL COMMAND
UNITED STATES AIR FORCE

NOTICE AND SIGNATURE PAGE

Using Government drawings, specifications, or other data included in this document for any purpose other than Government procurement does not in any way obligate the U.S. Government. The fact that the Government formulated or supplied the drawings, specifications, or other data does not license the holder or any other person or corporation; or convey any rights or permission to manufacture, use, or sell any patented invention that may relate to them.

Qualified requestors may obtain copies of this report from the Defense Technical Information Center (DTIC) (http://www.dtic.mil).

AFRL-RX-WP-JA-2015-0078 HAS BEEN REVIEWED AND IS APPROVED FOR PUBLICATION IN ACCORDANCE WITH ASSIGNED DISTRIBUTION STATEMENT.

//Signature//

PATRICK S. CARLIN, Project Engineer
Composite Materials and Processing Section
Composite Branch
Structural Materials Division

//Signature//

SEAN C. COGHLAN, Chief
Composite Materials and Processing Section
Composite Branch
Structural Materials Division

//Signature//

ROBERT T. MARSHALL, Deputy Chief
Structural Materials Division
Materials And Manufacturing Directorate

This report is published in the interest of scientific and technical information exchange and its publication does not constitute the Government's approval or disapproval of its ideas or findings.

REPORT DOCUMENTATION PAGE

Form Approved
OMB No. 0704-0188

1. REPORT DATE *(DD-MM-YY)*	2. REPORT TYPE	3. DATES COVERED *(From - To)*
February 2012	Interim	06 April 2010 – 17 January 2012

4. TITLE AND SUBTITLE
SEPARATING TEST ARTIFACTS FROM MATERIAL BEHAVIOR IN THE OXIDATION STUDIES OF HfB2-SiC AT 2000°C AND ABOVE (POSTPRINT)

5a. CONTRACT NUMBER
FA8650-10-D-5226-0002

5b. GRANT NUMBER

5c. PROGRAM ELEMENT NUMBER
62102F

6. AUTHOR(S)
Michael K. Cinibulk - AFRL/RXCC
Carmen M. Carney and Triplicane A. Parthasarathy - UES, Inc.

5d. PROJECT NUMBER
4347

5e. TASK NUMBER

5f. WORK UNIT NUMBER
X0L5

7. PERFORMING ORGANIZATION NAME(S) AND ADDRESS(ES)

AFRL/RXCC
2941 Hobson Way
Bldg 654, RM 136
Wright-Patterson AFB OH 45433

UES, Inc.
4401 Dayton-Xenia Rd.
Dayton, OH 45432-1894

8. PERFORMING ORGANIZATION REPORT NUMBER

9. SPONSORING/MONITORING AGENCY NAME(S) AND ADDRESS(ES)

Air Force Research Laboratory
Materials and Manufacturing Directorate
Wright-Patterson Air Force Base, OH 45433-7750
Air Force Materiel Command
United States Air Force

10. SPONSORING/MONITORING AGENCY ACRONYM(S)
AFRL/RXCCM

11. SPONSORING/MONITORING AGENCY REPORT NUMBER(S)
AFRL-RX-WP-JA-2015-0078

12. DISTRIBUTION/AVAILABILITY STATEMENT
Distribution Statement A. Approved for public release; distribution unlimited.

13. SUPPLEMENTARY NOTES
Journal article published in *Int. J. Appl. Ceram. Technol., 10 [2] 293–300 (2013).* Document contains color. The final publication is available at www.ceramics.org/ACT or http://onlinelibrary.wiley.com/doi/10.1111/j.1744-7402.2011.02730.x/abstract.

14. ABSTRACT
Oxidation characteristics of HfB_2-15 vol% SiC prepared by field-assisted sintering was examined at 2000°C by heating it in a zirconia-resistance furnace and by direct electrical resistance heating of the sample. Limitations of the material and the direct electrical resistance heating apparatus were explored by heating samples multiple times and to temperatures in excess of 2300°C. Oxide scales that developed at 2000°C from both methods were similar in that they consisted of a SiO_2/HfO_2 outer layer, a porous HfO_2 layer, and a HfO_2 layer depleted of SiC. But they differed in scale thicknesses, impurities present, scale morphology/complexity. Possible test artifacts are discussed.

15. SUBJECT TERMS
oxidation, UHTC, hafnium diboride, silicon carbide

16. SECURITY CLASSIFICATION OF:			17. LIMITATION OF ABSTRACT:	18. NUMBER OF PAGES	19a. NAME OF RESPONSIBLE PERSON (Monitor)
a. REPORT	b. ABSTRACT	c. THIS PAGE			Patrick S. Carlin
Unclassified	Unclassified	Unclassified	SAR	11	19b. TELEPHONE NUMBER *(Include Area Code)* (937) 904-5547

Int. J. Appl. Ceram. Technol., 10 [2] 293–300 (2013)
DOI:10.1111/j.1744-7402.2011.02730.x

International Journal of
Applied Ceramic TECHNOLOGY
Ceramic Product Development and Commercialization

Separating Test Artifacts from Material Behavior in the Oxidation Studies of HfB_2–SiC at 2000°C and Above

Carmen M. Carney* and Triplicane A. Parthasarathy

UES, Inc, Dayton, Ohio 45432

Michael K. Cinibulk

Air Force Research Laboratory, Materials and Manufacturing Directorate, Wright Patterson Air Force Base, Ohio 45433

Oxidation characteristics of HfB_2-15 vol% SiC prepared by field-assisted sintering was examined at 2000°C by heating it in a zirconia-resistance furnace and by direct electrical resistance heating of the sample. Limitations of the material and the direct electrical resistance heating apparatus were explored by heating samples multiple times and to temperatures in excess of 2300°C. Oxide scales that developed at 2000°C from both methods were similar in that they consisted of a SiO_2/HfO_2 outer layer, a porous HfO_2 layer, and a HfB_2 layer depleted of SiC. But they differed in scale thicknesses, impurities present, scale morphology/complexity. Possible test artifacts are discussed.

Introduction

Characterization of the oxide scale formed on ultra high temperature ceramics (UHTCs) has been a topic of intense study over the past decade. In particular, composite systems of diborides of hafnium or zirconium with SiC have been studied for their improved oxidation resistance compared with the diborides alone near 1600°C.[1–3] At temperatures below 1800–2000°C, a refractory porous metal oxide scale is formed that is protected by a glassy silica scale. However, as temperatures are increased the protective silica becomes less viscous and thus less protective. Hypersonic flight will require leading edges and nose cone components to withstand rapid heating and cooling to temperatures in excess of 2000°C under shear stresses imparted by air flow. In addition, the environment within the boundary layer near the component

This study was supported by the United States Air Force Contract # FA8650-10-D-5226.
*carmen.carney@wpafb.af.mil

will be comprised of a fraction of dissociated atoms depending on velocity, altitude, and other factors.[4,5] Dissociated oxygen can alter the boundary between active and passive oxidation of SiC and thus influence oxidation kinetics.[6] These temperatures and conditions are unattainable in traditional molybdenum disilicide element furnaces whereas conventionally accepted arc jet testing is expensive and the primary oxidant is dissociated oxygen, so new methods of testing have been developed. Methods such as oxyacetylene torch heating,[7–9] laser heating,[10] direct resistance heating of the sample itself,[11–13] and scramjet simulators[14] are being developed. The rapid heating profiles and higher temperatures attainable with these tests may lead to different oxide morphologies and performance than those observed with furnace-heated samples. It is imperative that a correlation between different testing methods is made so that samples prepared by different exposure methods may be compared. To this end, HfB_2–SiC samples were heated in air at 2000°C using a zirconia-resistance furnace and direct resistance heating of the sample and the resulting oxidation products were compared. In addition, the limits of resistance heating including multiple cycles and maximum temperatures were examined.

Experimental Procedure

Commercially available HfB_2 (Materion, Milwaukee, WI, 99.9%, 45 μm) and β-SiC (Materion, 99.9%, 1 μm) were used to prepare HfB_2-15 vol% SiC (HS). The powder mixtures were ball milled in isopropanol for 24 h with SiC grinding media, dried at room temperature, and subsequently dry milled for 12 h. Typical weight loss of the SiC grinding media after milling was 0.2 mg (0.2 wt% of the total batch). The powders were sieved through an 80-mesh (177 μm) screen.

A quantity of 150 g of the milled powders was loaded into a 60-mm diam. graphite die. A layer of BN and graphite foil separated the powder from the die with the powder in contact with the graphite foil. The powder-filled dies were cold pressed at approximately 50 MPa. The powders were sintered using field-assisted sintering (FAS: HPD 25-1, FCT Systeme, Rauenstein, Germany) at 2000°C for 15 min under a 32 MPa load. The controlled heating and cooling rates were 50°C/min. The load was applied during heating to 1600°C and released on cooling to 1000°C.

Oxidation samples were cut with a wire electro-discharge machine (EDM) into 5 mm × 5 mm × 3 mm rectangles (furnace heating) and 53 mm × 3.5 mm × 5.0 mm rectangles with a centered 19–25 mm long 3 mm thick region of reduced area (resistance heating). The samples were polished using diamond slurry to a 1 μm finish.

Polished samples were heated by a zirconia-resistance furnace (ZrF-25: Shinagawa Refractories, Tokyo, Japan) and direct electrical resistance. Macrographs of the two tests and sample geometry are shown in Fig. 1. The furnace heating was accomplished by a molybdenum disilicide pre-heater to 1100°C and a zirconia element to 2000°C at a rate of 5°C/min. The samples were held at temperature for 30 min. Temperature measurements were performed using a single color pyrometer focused on the zirconia element. Samples were supported on a zirconia crucible. The zirconia crucibles were cut from a larger crucible (Advalue, Tuscon, AZ; 10 mL Ca-stabilized ZrO_2 crucible; 95% ZrO_2 and 4 ± 1% Ca). Direct electrical resistance heating was controlled by the power output of an AC power supply across the sample and temperature was read by a two-color pyrometer (FMP2; FAR Associates, Macedonia, OH) that was focused on the center of the reduced-thickness area. The samples were held in place between two graphite spacers by tightening set screws on the copper electrodes. Ag paint was used on the ends of the samples to improve electrical contact. Temperature, current, and voltage data were recorded using LabVIEW (National Instruments, Austin, TX). Table I lists the oxidized samples with their heating conditions.

Oxidized samples were mounted in epoxy and polished in cross section perpendicular to the bottom (side facing the crucible or notched side) of the sample to a 1 μm finish using diamond slurry. The microstructures were characterized using scanning electron microcopy (SEM, Quanta, FEI, Hillsborough, OR) along with energy dispersive spectroscopy (EDS, Pegasus 4000; EDAX, Mahwah, NJ) for elemental analysis. All EDS analysis was done using 15 kV accelerating voltage and at least a 100 s live capture time.

Results

Single 2000°C Exposure

The heating profiles of the HfB_2-15 vol% SiC zirconia-resistance furnace heated sample (HS-F) and

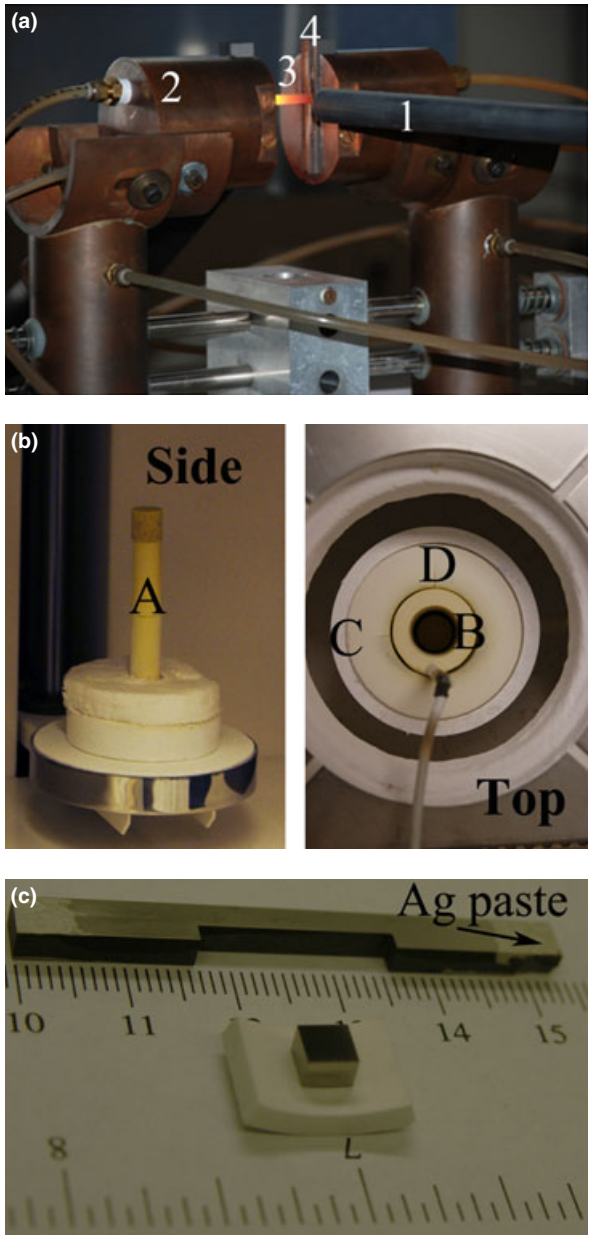

Fig. 1. (a) Macrograph of direct electrical resistance heating apparatus. The temperature is read by means of a fiber optic cable through a carbon tube (1) that leads to the pyrometer. Power is supplied through the copper electrodes (2) to a heated sample (3) gripped by carbon spacers (4). (b) Macrograph of the zirconia-resistance furnace showing the sample stand (A), cylindrical zirconia heating element (B), alumina insulation (C), and molybdenum oxide insulation (D). (c) Samples prepared for direct electrical heating (top) and zirconia-resistance heating (bottom) on the supporting zirconia crucible. The Ag paste improves electrical conduction.

direct electrical resistance-heated (HS-R) sample are shown in Fig. 2a and b, respectively. The maximum observed temperature of the HS-R sample was 2027°C using 82.5 V and 20.3 A (averaged over the hold). The oxidized HS-F sample had a thicker oxide scale (Fig. 3a) compared to the HS-R sample (Fig. 3b). The HS-F sample was exposed to oxidizing temperatures for a greater length of time than the HS-R sample (6.5 h above 1100°C compared to ~4 min above 800°C). The oxide layers labeled in Fig. 3a (HS-F) and Fig. 3b (HS-R) are composed of (I) a SiO_2-based glass that penetrates a HfO_2-based skeleton; (II) a porous HfO_2 scale; and (III) a SiC-depleted layer. The SiC-depleted layer is defined as HfB_2 with a reduced SiC content (partially oxidized SiC). The average total oxide scale thickness measured from the top side of the HS-F sample is 660 ± 45 μm with the depleted layer comprising 53% of the scale. The thickest total oxide scale measured on the HS-R sample was 105 μm with 5% of the total scale consisting of the depleted layer.

The oxide scales of HS-F samples possess a distinct two-phase SiO_2-based glass with the less-pure (less viscous) impurity-laden glass rising to the surface of the oxide scale and the purer glass found deeper within the scale (Fig. 4a). A two-phase glass found in furnace heating has been described previously by the authors, which was shown to contain Al and Ca as major impurities.[15] In addition, $HfSiO_4$ (with a Ca impurity) is found in the HS-F sample, but not the HS-R sample. The existence and absence of $HfSiO_4$ was confirmed by XRD. Figure 4b is an EDS comparison of the purer (darker) and impure (lighter) glasses in the HS-F sample along with the $HfSiO_4$ and HfO_2 phases. In the HS-R sample Al impurities can be found randomly distributed throughout the glassy phase (inset Fig. 4c). Figure 4d is a representative EDS spectra of different locations within the HS-R glass. There is no hierarchy to the concentration of Al in the glass phase when comparing the chemistry of the glass along the length of the HS-R oxide scale.

Repeated 2000°C Exposure

An advantage of the direct electrical resistance heating test is that the sample can be exposed multiple times to the same or different heating profiles. A sample (HS-Rr) was heated to 2000°C twice using the same heating profile as HS-R. The maximum observed temperature was 2030°C. The heating profile and a

Table I. List of the Oxidized HfB_2-15 vol% SiC Samples and their Heating Conditions

Sample ID	Test method	Max. observed temp. (°C)	Hold time (min)	Comments
HS-F	Furnace	2000	30	—
HS-R	Self-heating	2027	1	—
HS-Rr	Self-heating	2030	1	Two 1 min holds
HS-R2	Self-heating	2041	2	—
HS-Rf	Self-heating	2325	0	Heated to failure

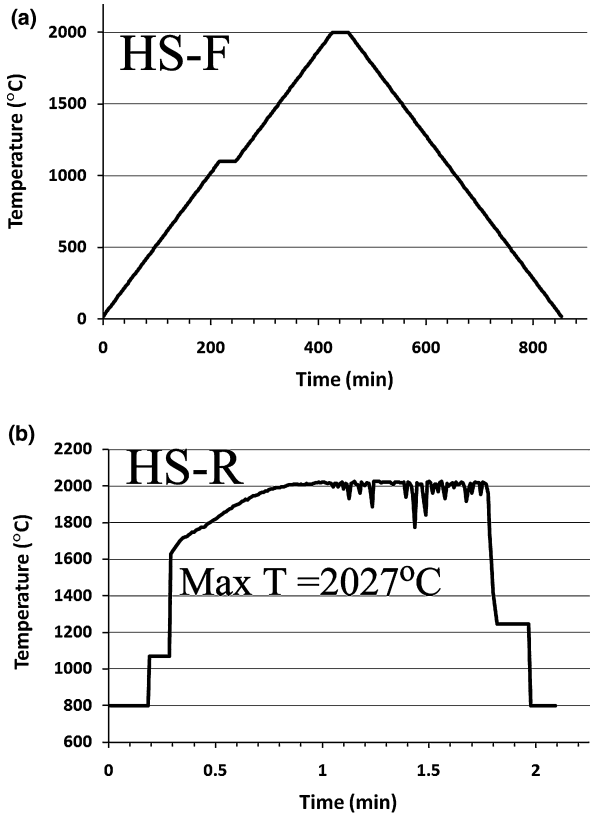

Fig. 2. Heating profiles of the (a) HS-F (calculated) and (b) HS-R (actual) samples.

micrograph of the resulting oxide scale are shown in Figs. 5a and b. The oxide scale has a periodic structure consisting of layers of SiO_2 and HfO_2 penetrated by SiO_2. For comparison, a sample (HS-R2) was heated to 2000°C for 2 min. (Fig. 5c) with a maximum observed temperature of 2040°C. The thickest measured oxide scale of the HS-R2 sample was double that found for the HS-R sample (217 vs 105 μm), and the oxide scale was not composed of periodic layers. The

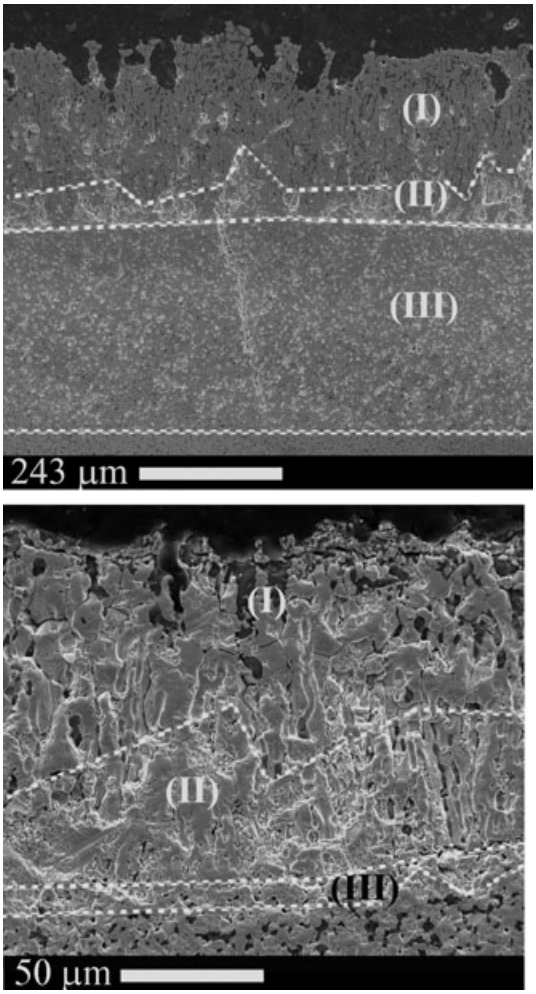

Fig. 3. (a) Micrograph of the HS-F sample after oxidation at 2000° C (b) Micrograph of the HS-R sample after oxidation at ~2000° C. The oxide layers are (I) HfO_2 penetrated by SiO_2, (II) porous HfO_2, and (III) depleted HfB_2 layer. The approximate boundary between layers is shown by the dashed white lines.

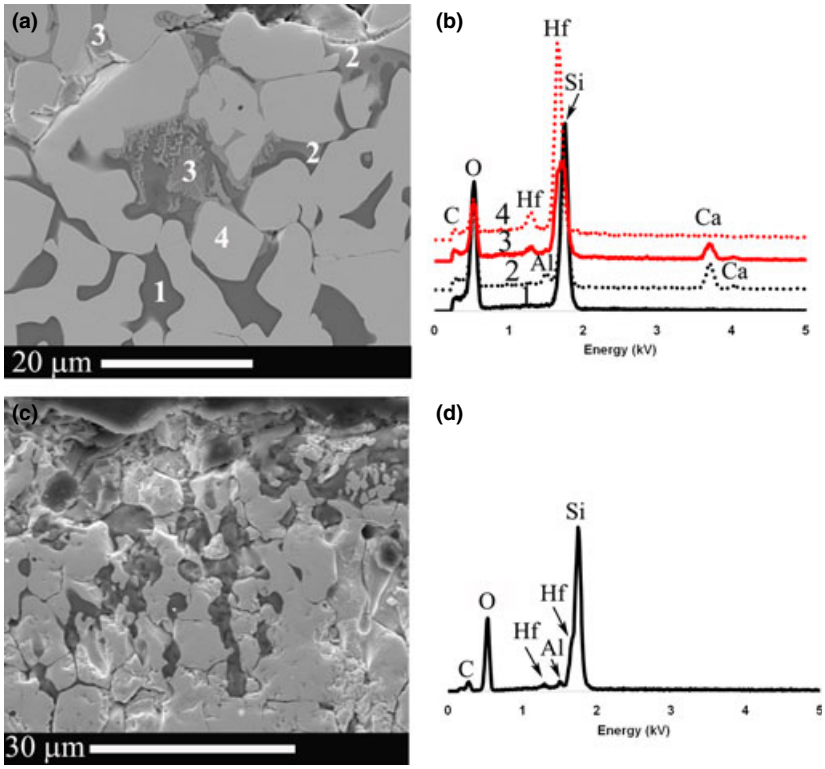

Fig. 4. (a) Micrograph showing the different phases found in the HS-F oxide scale (1) SiO_2, (2) Si–Al–O, (3) $HfSiO_4$ with Ca, and (4) HfO_2; (b) EDS corresponding to the phases found in (a); (c) Micrograph showing the HfO_2 (light) and Si–O–Al (dark) phases found in the HS-R oxide scale; (d) representative EDS of the Si–Al–O phase corresponding to (c).

oxide scale formed near the center of the reduced area on the HS-Rr and HS-R2 samples were nonadherent. Cracks were also observed within the depleted layer of the HS-F sample and at the interface between HfO_2 and the SiC-depleted layer (Fig. 3a). In the HS-R sample, fracture is observed between the depleted layer and the HfO_2 layer at the center of the sample (Fig. 3b), whereas adherent oxide scales exist near the end of the reduced area.

Temperatures Beyond 2000°C

The maximum temperature of the direct resistance test is limited only by the available power and the survivability of the sample. A sample (HS-Rf) was heated to failure, where failure was defined as the sample fracturing such that the electrical path was disrupted. The maximum observed temperature was 2325°C. A micrograph of the cross section of the HS-Rf sample (Fig. 6) reveals extensive internal damage. Large pores are found inside the sample whereas an oxide scale covers the surface. The bulk unoxidized material from the center of the sample (inset Fig. 6) was confirmed by EDS to be SiC and HfB_2. The microstructure suggests formation of a liquid phase, which is consistent with the calculated eutectic at 2347°C in the HfB_2–SiC system.[16] The oxide scale (inset Fig. 6) is composed of HfO_2 penetrated by SiO_2. Meng *et al.*[13] similarly showed the failure of a ZrB_2–SiC sample at temperatures above 2300°C (2207°C eutectic temperature[16]), but did not show any micrographs of the interior microstructure.

Discussion

The direct comparison of the zirconia-resistance heated and direct electrical resistance-heated HfB_2–SiC samples at 2000°C provide insight to the limitations of furnace heating. Due to slower heating rates and contamination from contact between the sample and

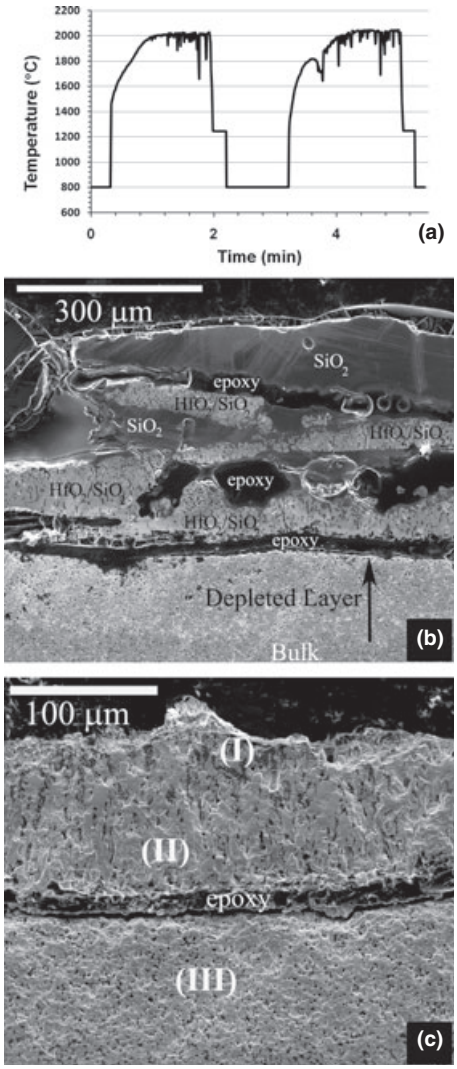

Fig. 5. (a) Heating profile of sample HS-Rr. (b) Micrograph of the oxide found in hottest region of the oxidized HS-Rr sample heated to 2000°C for 1 min two times. (c) Micrograph of the oxide found in hottest region of the oxidized HS-R2 sample heated to 2000°C for two minutes. The layers are the same as those found in the HS-R sample: (I) HfO_2 penetrated by SiO_2, (II) porous HfO_2, and (III) depleted HfB_2.

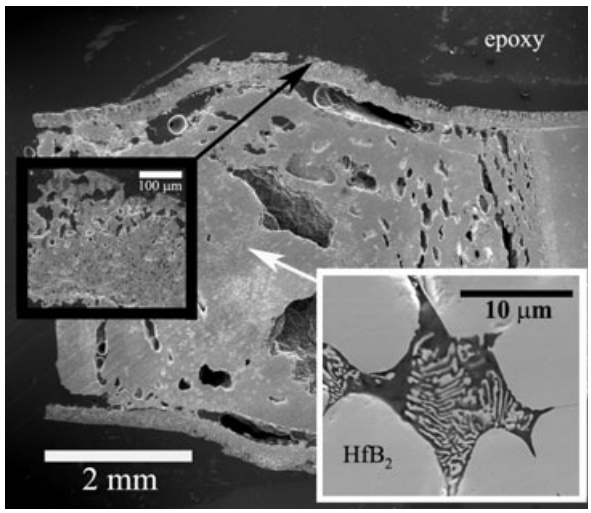

Fig. 6. Micrograph of the HS-Rf sample heated to 2325°C. The white-outlined inset shows HfB_2 grains (labeled) and the eutectic SiC (dark)–HfB_2 (light) structure found in the interior of the sample. The black-outlined inset is the oxide scale composed of HfO_2 and SiO_2 found on the exterior of the HS-Rf sample.

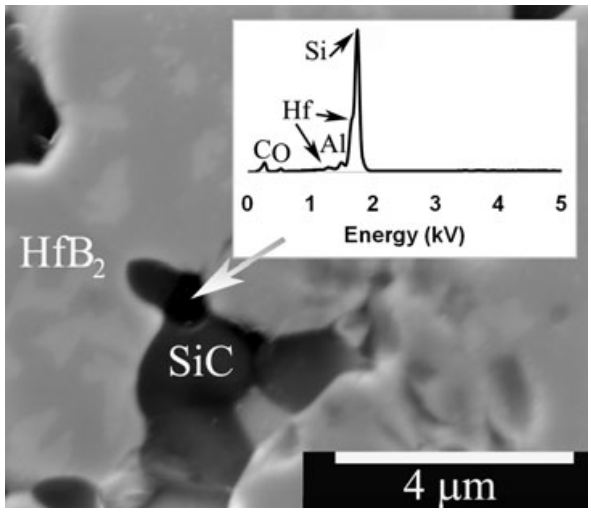

Fig. 7. Micrograph showing a Si–Al–O impurity phase in the bulk of the HfB_2-15 vol% SiC sample. The C signal in the EDS (inset) is from the carbon coating applied to the sample.

crucible, the HS-F total oxide scale thickness is greater than that observed in the HS-R sample. The difference in heating rates can also explain the observation of $HfSiO_4$ in the HS-F sample but not in the HS-R sample. $HfSiO_4$ is only stable below ~1726°C,[17,18] therefore; its formation in the HS-F sample could occur during slow cooling. HfO_2 and SiO_2 form an incongruently melting silicate and thus require solid-state diffusion to form the silicate phase adding an extra kinetic limitation on its formation.[17] The rapid heating and cooling rates of the HS-F sample presumably do not allow for the separation of glasses with different viscosities or for the formation of $HfSiO_4$.

In addition, the lack of Ca impurity in the resistance-heated sample suggests the source of the impurity to be the CaO-stabilized zirconia crucible or zirconia heating element, whereas the presence of Al in both samples implies that it is an inherent impurity in the starting powders. For comparison, a HfB_2–SiC sample was heated in the zirconia-resistance furnace using a Y_2O_3-stabilized zirconia crucible. The glass near the contact region of the sample and crucible was found to contain Si, Al, Ca, Y, and O. Since the crucible was reported to only contain 0.001% Ca, the zirconia sample stand (Part A in Fig. 1) was the likely source of Ca in this test. The HfB_2 and SiC powders are reported by the manufacturer to contain 0.03% and 0.01% Al, respectively. Figure 7 is a micrograph showing the SiC grains with a pocket of impurities in the as-processed material. These areas can be found throughout the sample adjacent to SiC grains and are shown by EDS (inset) to contain Si, Al, and O. The slow heating rates and contact contamination issues of the zirconia element furnace are not expected in hypersonic flight conditions and serve to complicate the analysis of UHTC oxidation resistance testing.

When a HfB_2–SiC sample is heated by direct electrical resistance through multiple heating and cooling cycles, spallation of the oxide scale is suggested by the presence of the repeating SiO_2–HfO_2 layers. Such layered oxide structures have not been reported for furnace-heated samples and was not observed in a sample heated for the same time (HS-R2) with a single heating and cooling cycle. There are two sources of stress during oxidation that may lead to fracture during temperature changes: (i) thermal expansion mismatch and (ii) volume changes associated with phase transformations. The coefficient of thermal expansion (CTE) of HfO_2 depends on the impurity content and phase, but typical values are 5×10^{-6} to 7×10^{-6} K^{-1} for room temperature to 1250°C with purer HfO_2 having lower values.[19,20] Gasch *et al.*[21] measured the CTE of pure HfB_2, pure SiC, and a combination of HfB_2-20 vol% SiC to find that the CTE of HfB_2-20 vol% SiC was $\sim 5 \times 10^{-6}$ K^{-1} at room temperature and $\sim 7 \times 10^{-6}$ K^{-1} at 1600°C and fell between the CTE values of pure HfB_2 (higher) and SiC (lower) as expected by the rule of mixtures. The transformation of HfO_2 from monoclinic to tetragonal upon heating (10% conversion at 1642°C) or tetragonal to monoclinic during cooling (10% conversion at 1710°C),[18,22,23] is accompanied by a 3–3.5% volume contraction/expansion upon heating/cooling.[22,24] This volume expansion could lead spallation of the oxide scale.

As the absolute CTE and modulus of the multiphase oxide scale are not known at elevated temperatures, the main contributing factor to oxide spallation cannot be identified definitively. However, if it is assumed that the volume expansion upon phase transformation is isotropic then at minimum the linear expansion due to phase transformation would be 1%. To achieve greater than 1% linear expansion from 2000°C to room temperature when compared to the bulk, the difference in CTE of the oxide scale and bulk would need to surpass $\sim 4 \times 10^{-6}$ K^{-1}. The reported range of CTE values for the bulk HfB_2–SiC and HfO_2 allow for a $\sim 2 \times 10^{-6}$ K^{-1} difference between the CTE values, but the difference could increase at higher temperatures. Therefore, it is possible that the phase transformation and CTE mismatch both contribute to spallation of the oxide scale. The role of CTE mismatch and HfO_2 phase transformation on oxide scale adherence deserve further study.

The limitation of the resistance heater was explored as the sample was heated to failure above 2300°C. The entire sample was soaked at the elevated temperature allowing for the formation of the HfB_2–SiC liquid phase inside the HS–Rf sample. Furthermore, the temperature may be greater in the interior because the oxide scale will not be electrically conductive and is an effective thermal insulator. Under flight conditions, only the outer regions of the sample would be heated and the high thermal conductivity of the diboride phase would lead to a temperature gradient through the thickness of the component. A temperature gradient is experienced along the length of the direct electrical resistance sample and can provide insight to oxide and bulk microstructures over a temperature range.

Conclusion

Temperatures up to 2000°C can be achieved in a laboratory furnace; however, these tests suffer from slow heating profiles and potential interactions between furnace materials and the sample being tested. The observation of Ca and $HfSiO_4$ in the oxide scale affects the glass properties, but this is not expected in a flight environment. The use of resistance heating allows noncontact testing with a high heating profile. Features like fracture between the oxide scale and the depleted layer

and Al impurities are universal observations between both heating tests and require further investigation. In addition, research to stabilize the tetragonal transformation may aid in a more adherent scale. Resistance heating may be further utilized to study multiple heating profiles and test materials for scale adherence. The resistance testing is limited by the uniform heating of the sample that would not be expected in a real flight environment. Further comparison of test methods such as laser heating, oxyacetylene torch testing, or scramjet testing would be beneficial to understanding material properties.

Acknowledgments

The authors thank David Hart, AFRL Air Vehicles Directorate, for his assistance with the resistance heater operation and Sindhura Gangireddy, University of Michigan, for the discussion involving microstructures of resistively heated ZrB_2–SiC to parallel our own observations.

References

1. J. R. Fenter, "Refractory Diborides as Engineering Materials," *SAMPE Q*, 2 1–15 (1971).
2. J. W. Hinze, H. C. Tripp, and W. C. Graham, "High-Temperature Oxidation Behavior of a HfB_2 Plus 20 v/o SiC Composite," *J. Electrochem. Soc.*, 122 [9] 1249–1254 (1971).
3. W. C. Tripp, H. H. Davis, and H. C. Graham, "Effect of an SiC Addition on the Oxidation of ZrB_2," *Ceram. Bull.*, 52 [8] 612–616 (1973).
4. D. M. Van Wei, D. G. Drewry, D. E. King, and C. M. Hudson, "The Hypersonic Environment: Required Operating Conditions and Design Challenges," *J. Mater. Sci.*, 39 [19] 5915–5924 (2004).
5. T. H. Squire and J. Marschall, "Material Property Requirements for Analysis and Design of UHTC Components in Hypersonic Applications," *J. Eur. Ceram. Soc*, 30 [11] 2239–2251 (2010).
6. A. Bongiorno, *et al.* "A Perspective on Modeling Materials in Extreme Environments: Oxidation of Ultrahigh-Temperature Ceramics," *MRS Bull.*, 31 [5] 410–418 (2006).
7. T. Sufang, J. Deng, S. Wang, W. Liu, and K. Yang, "Ablation Behaviors of Ultra-High Temperature Ceramic Composites," *Mater. Sci. Eng. A*, 465 [1–2] 1–7 (2007).
8. E. L. Corral and L. S. Walker, "Improved Ablation Resistance of C-C Composites Using Zirconium Diboride and Boron Carbide," *J. Eur. Ceram. Soc*, 30 [11] 2357–2364 (2010).
9. J. Han, P. Hu, X. Zhang, S. Meng, and W. Han, "Oxidation-Resistant ZrB2–SiC Composites at 2200 °C," *Comp. Sci. Technol.*, 68 799–806 (2008).
10. D. D. Jayaseelan, H. Jackson, E. Eakins, P. Brown, and W. E. Lee, "Laser Modified Microstructures in ZrB_2, ZrB_2/SiC and ZrC," *J. Eur. Ceram. Soc.*, 30 [11) 2279–2288 (2010).
11. S. N. Karlsdottir and J. W. Halloran, "Rapid Oxidation Characterization of Ultra-High Temperature Ceramics," *J. Am. Ceram. Soc.*, 90 [10] 3233–3238 (2007).
12. Z. Wang, Z. Wu, and G. Shi, "The Oxidation Behaviors of ZrB_2-SiC-ZrC Ceramic," *Solid State Sci.*, 13 [3] 534–538 (2010).
13. S. Meng, C. Liu, G. Liu, G. Bai, C. Xu, and W. Xie, "Mechanisms of Material Failure for Fast Heating up at the Center of Ultra High Temperature Ceramic," *Solid State Sci.*, 12 [4] 527–531 (2010).
14. T. A. Parthasarathy, M. D. Petry, G. Jefferson, M. K. Cinibulk, T. Mathur, and M. R. Gruber, "Development of a Test to Evaluate Aerothermal Response of Materials to Hypersonic Flow Using a Scramjet Wind Tunnel," *Int. J. Appl. Ceram. Technol.*, 8 [4] 832–847 (2011).
15. C. M. Carney, "Oxidation Resistance of Hafnium Diboride-Silicon Carbide From 1400 to 2000°C," *J. Mater. Sci.*, 44 [20] 5673–5681 (2009).
16. L. Kaufman, "Calculation of multicomponent refractory composite phase diagrams," NSWC TR 86-242 1 June 1986.
17. J.-H. Lee, "Ternary Phase Analysis of Interfacial Silicates Grown in HfO_x/Si and Hf/SiO_2/Si Systems," *Thin Solid Films*, 472 [1–2] 317–322 (2005).
18. S. V. Ushakov, A. Navrotsky, Y. Yang, S. Stemmer, K. Kukli, M. Ritali *et al.*, "Crystallization in Hafnia- and Zirconia-Based Systems," *Phys. Status. Solidi*, 241 [10] 2268 (2004).
19. S. L. Dole, O. Hunter, F. W. Calderwood, and D. J. Bray, "Microcracking of Monolithic HfO_2," *J. Am. Ceram. Soc*, 61 [11–12] 486–490 (1978).
20. S. R. Skaggs, "Zero and Low Coefficient of Thermal Expansion Polycrystalline Oxides," LA-6918-MS September 1977.
21. M. Gasch, D. Ellerby, E. Irby, S. Beckman, M. Gusman, and S. Johnson, "Processing, Properties and Arc Jet Oxidation of Hafnium Diboride/Silicon Carbide Ultra High Temperature Ceramics," *J. Mater. Sci.*, 39 [19] 5925–5937 (2004).
22. X. Luo, W. Zhou, S. V. Ushakov, A. Navrotsky, and A. A. Demkov, "Monoclinic to Tetragonal Transformations in Hafnia and Zirconia: A Combined Calorimetric and Density Functional Study," *Phys. Rev. B*, 80 134119 (2009).
23. G. M. Wolten, "Diffusionless Phase Transformations in Zirconia and Hafnia," *J. Am. Ceram. Soc.*, 46 [9] 418–422 (1963).
24. L. Kaufman, E. V. Clougherty, and J. B. Berkowitz-Mattuck, "Oxidation Characteristics of Hafnium and Zirconium Diboride," *Trans. Metall. Soc. AIME*, 239 458–466 (1967).